Scaling mobility patterns and collective movements: Deterministic walks in lattices

Xiao-Pu Han,[1] Tao Zhou,[1,2,*] and Bing-Hong Wang[1,3]

[1]*Department of Modern Physics, University of Science and Technology of China, Hefei 230026, People's Republic of China*

[2]*Web Sciences Center, University of Electronic Science and Technology of China, Chengdu 610051, People's Republic of China*

[3]*Research Center for Complex System Science, University of Shanghai for Science and Technology, Shanghai 200093, People's Republic of China*

(Received 26 November 2010; revised manuscript received 8 April 2011; published 10 May 2011)

Scaling mobility patterns have been widely observed for animals. In this paper, we propose a deterministic walk model to understand the scaling mobility patterns, where walkers take the least-action walks on a lattice landscape and prey. Scaling laws in the displacement distribution emerge when the amount of prey resource approaches the critical point. Around the critical point, our model generates ordered collective movements of walkers with a quasiperiodic synchronization of walkers' directions. These results indicate that the coevolution of walkers' least-action behavior and the landscape could be a potential origin of not only the individual scaling mobility patterns but also the flocks of animals. Our findings provide a bridge to connect the individual scaling mobility patterns and the ordered collective movements.

DOI: 10.1103/PhysRevE.83.056108 PACS number(s): 89.75.Fb, 05.40.Fb, 89.75.Da

I. INTRODUCTION

Recently, the scaling properties in mobility patterns of animals have attracted increasing attention [1]. The traditional scenario about the "nearly random walks" of animals is now challenged by the cumulated empirical observations, which indicate heavy-tailed displacement distributions approximated to a power-law form $P(l) \sim l^{-\alpha}$. Examples include the foraging process and daily movements of wandering albatrosses [2], honeybees [3,4], spider monkeys [5], microzooplanktons [6], marine predators [7], and so on. These widespread observations imply some general mechanisms underlying animals' mobility patterns.

Interpretations of the animals' mobility patterns can be divided into two classes. One is the *optimal search strategies* [8–11], which indicate that animals can maximize the searching efficiency by using power-law movements. Another is the *deterministic walks* (DW) [12–15], where a number of prey are randomly distributed on a field and a walker will continuously catch the nearest prey from the current position. Recent studies introduced many real-life factors into the standard framework of DW, such as olfactory-driven foraging [16] and complex environment effects [17]. In addition, Kamimura and Ohira [18] studied the group chasing-escaping process with active targets, which displays many complex mobility behaviors, such as the game of different moving strategies of chasers and the self-organized spatial structures.

To uncover the origin of scaling properties in animal mobility, we propose a variant DW model that takes into account the regeneration of resources in a landscape and the least-action movements. Our model can reproduce the power-law distribution of displacements and the scaling behavior in probability density of having moved a certain distance at a certain time, agreeing well with the empirical observations. In addition, our model generates ordered collective movements of walkers with a quasiperiodic synchronization of walkers' directions, indicating that the coevolution of walkers' least-action behavior and the landscape could be a potential origin of not only the individual mobility patterns but also the population of flocks.

II. MODEL

Food resources in the real environment can regenerate by themselves as the growth and propagation of plants and prey, until reaching a natural limitation of abundance. The maximization of foraging benefits and minimization of costs (e.g., the least-action movements) usually underlie the animals' behavior. Our model takes into account these two fundamental ingredients. The environment is represented by two-dimensional $N \times N$ lattices with nonperiodic boundary conditions (i.e., walkers cannot go across the boundary), and each lattice has prey resource $V(i,j)$ [for the lattice at coordinate (i,j)]. The maximum prey resource in each lattice is set as a fixed value V_m. Different from the standard DW, a more realistic case with multiple walkers (the number of walkers is denoted by M) is considered in our model. The updating rules about the landscape and walkers' positions are as follows.

(i) At each time step, each walker chooses the nearest lattice with the maximum prey resource to occupy at the next time step, and if there is more than one possible choice, the walker will randomly select one (see Fig. 1). The movement is treated as instantaneous, namely, the diversity of velocity is ignored. The displacement (i.e., moving length) l is defined as the geometric distance from the current occupied lattice to the next occupied lattice, namely, $l = \sqrt{(x_1 - x_0)^2 + (y_1 - y_0)^2}$, where the coordinates (x_0, y_0) and (x_1, y_1) denote the current position and the next position of the walker, respectively.

(ii) The resource V in the current occupied lattice of the walker is exhausted by the walker, namely, $V \leftarrow 0$.

(iii) For each lattice with $V < V_m$ (currently not occupied by a walker), the resource increases a unit at each time step until $V = V_m$, representing the regeneration of prey resources.

(iv) When the number of walkers $M > 1$, walkers update their positions with random order asynchronously according to the above algorithms at each time step.

*zhutou@ustc.edu

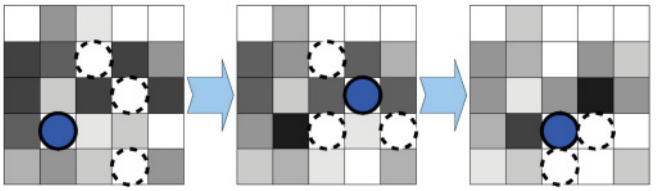

FIG. 1. (Color online) Illustration of the movement of a walker in three successive time steps, where the blue filled circle denotes the current position of the walker and the white dashed circles denote all the possible positions in the next time step. The values of V in lattices are denoted by different shades of gray, with white for $V = V_m$ and black for $V = 0$.

Because the resource in each lattice regenerates with a fixed speed and each walker consumes at most V_m resource at each time step, we define $r = MV_m/S$ to express the ratio between the total consumption of walkers and the total regeneration speed of prey resource in the landscape, where $S = N \times N$ is the area of the landscape. When $r = 1$, the consumption of prey resource is equal to the regeneration speed, and the resource is in a critical status. However, if $r < 1$, the system has redundant resources. In our simulations, M and r are tunable parameters, and the value of V_m is determined by $V_m = rS/M$. Given M and r, the results of our model do not depend on the value of V_m and thus are comparable.

Note that the movements in our model are not purely "deterministic" when $r < 1$ or $M > 1$. This probabilistic property comes from two sources: One is the random order in updating walkers' positions when $M > 1$; the other is that a walker may have more than one choices for the next position. Purely deterministic cases appear only when $r = 1$ and $M = 1$, in which the landscape has only one lattice with V_m resource and the walker has to periodically repeat its earlier trajectories. In cases when $r = 1$ and $M > 1$, although it is possible that walkers exchange their trajectories under the treatment with random order, the visited time on each lattice is still strict periodic if V_m is an integer.

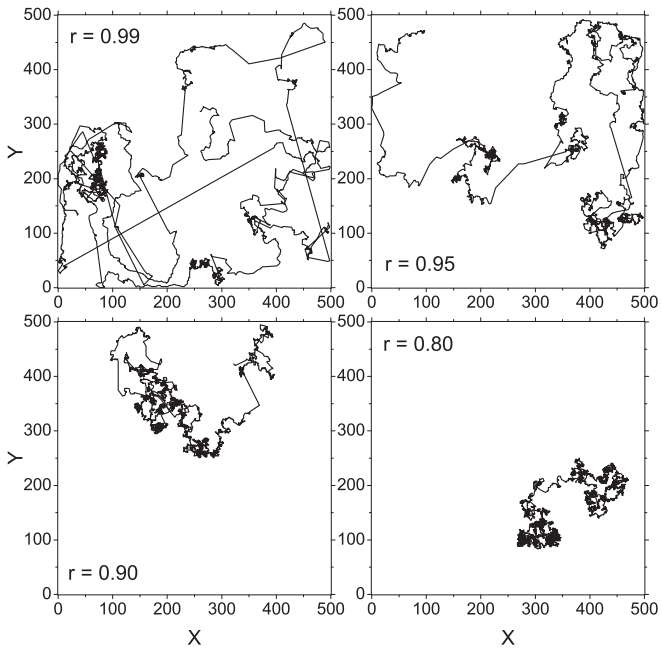

FIG. 2. The trajectories of a walker in 5000 consecutive steps for different r. Other parameters are $M = 100$ and $N = 500$.

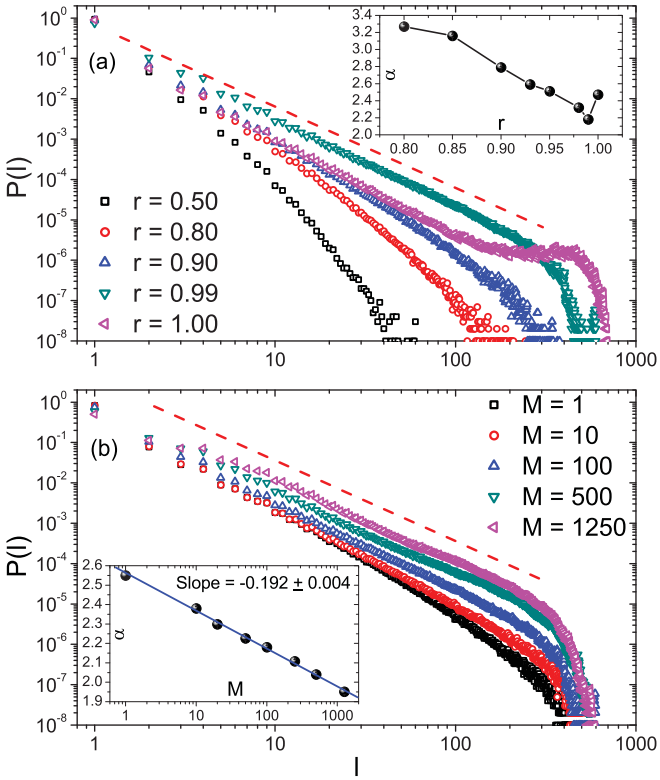

FIG. 3. (Color online) (a) Move length distribution $P(l)$ for different r, where the inset shows the dependence between the power-law exponent α and r. Other parameters are $M = 100$ and $N = 500$. (b) $P(l)$ for different M, where the inset shows the dependence between α and M, and the blue line denotes the fitting line with a slope of -0.192. Other parameters are $r = 0.99$ and $N = 500$. The red dashed lines in the plots represent a power law with an exponent of -2. All the data points are averaged over 100 independent runs, each of which includes 10^6 movements. The size of the error bars in the insets is smaller than the data points.

III. MOVE LENGTH DISTRIBUTION

In our simulations, the size of the landscape is fixed as $N = 500$. We assume the prey resource is full before a group of animals comes into the habitat; thus, we set the initial prey resource of each lattice to be V_m, and the initial positions of walkers are randomly distributed in the landscape. Except for the case of $r = 1$, our simulations show that the move length distribution (MLD) becomes stable after the evolution of $\frac{S}{(1.0-r)M}$ time steps, so our statistics take into account the walkers' movement after $\frac{S}{(1.0-r)M}$ time steps. When $r = 1$, the number of lattices having maximum resource is equal to the number of walkers M in the steady state. In this case, each walker has to repeat its early trajectory or other walkers' trajectories after the first S/M time steps (after that time, the consumption equals regeneration), so our statistics take into account the walkers' movement after S/M time steps .

Figure 2 shows the trajectories of a walker for different r, where abundant long-range movements can be observed when

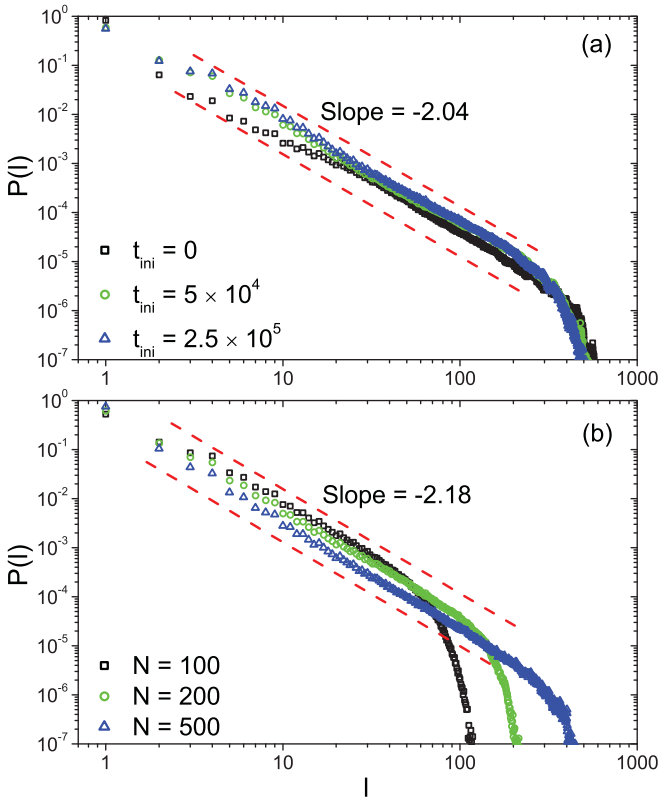

FIG. 4. (Color online) (a) MLD in different time stages. Simulations were run for $r = 0.99$, $M = 500$, and $N = 500$, where black squares, green circles, and blue triangles stand for the stages starting from initial time $t_{\text{ini}} = 0$, 5×10^4, and 2.5×10^5, respectively. The time duration in each of the stages is 2000 steps. The parallel red dashed lines denote the power law with a slope of -2.04, which corresponds to the fitting value of the curve $t_{\text{ini}} = 5 \times 10^4$. (b) MLD for different landscape sizes N. Simulations were run for $r = 0.99$, $M = 100$. The parallel red dashed lines denote the power law with a slope of -2.18, which corresponds to the fitting value of the curve $N = 500$. All the data points are averaged over 100 independent runs.

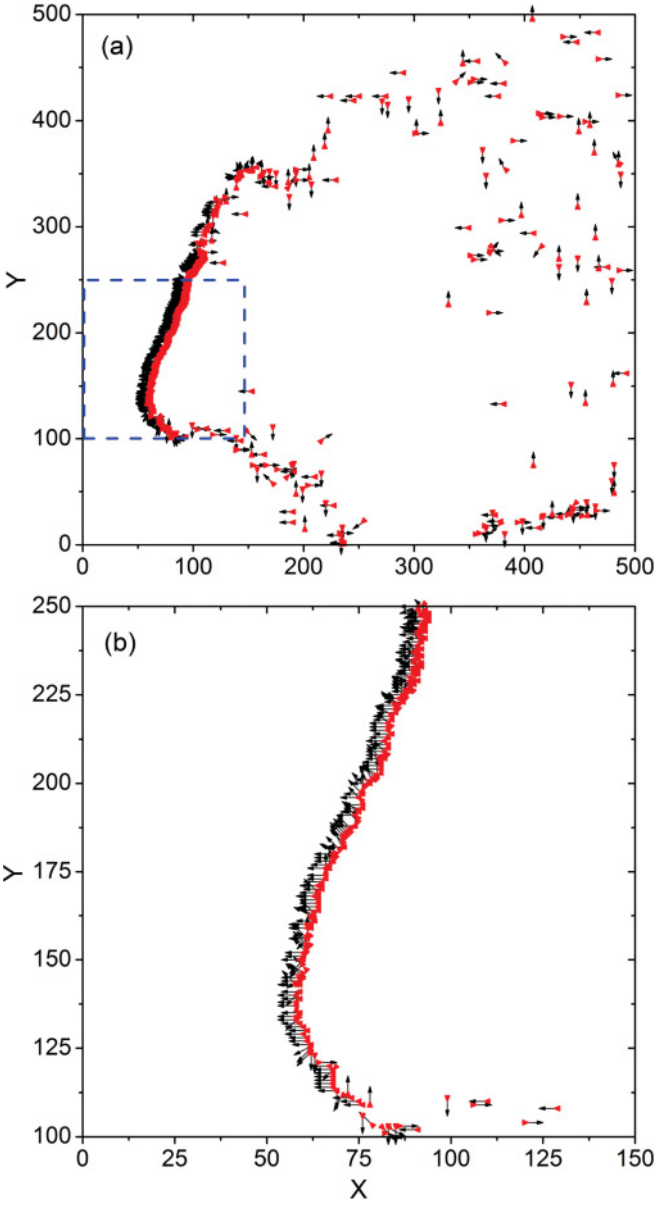

FIG. 5. (Color online) (a) A typical ordered marching band of walkers generated by our model when $t = 60\,335$ ($\psi = 0.60$). The red triangles and black arrows denote the current positions and directions of walkers, respectively. The parameters are $r = 0.99$, $M = 500$, and $N = 500$. (b) Enlargement of the front of the marching band in the blue dashed square in (a).

r approaches 1. The MLD $P(l)$ for different r and M are shown in Figs. 3(a) and 3(b), respectively. When r approaches 1, a scaling property of the move length distribution, say $P(l) \sim l^{-\alpha}$, can be observed. The analytical result for the MLD is given in the Appendix, which agrees with the simulations. As mentioned above, when $r = 1$, the trajectory is periodic, and thus, at the last time step of a period, the walker returns to its origin, corresponding to a generally long displacement with the same order of the system size. Therefore, as shown in Fig. 3(a), when $r = 1$, a peak appears at $l \approx N = 500$. The dependence between the power-law exponent α and the parameters r and M are shown in the insets of Figs. 3(a) and 3(b), respectively. Except for $r = 1$, α decreases monotonously with increasing r. For example, when $M = 100$, α decreases from 3.3 to 2.2 when r changes from 0.80 to 0.99. This range of α covers almost all the known real-world observations of MLD of animals. This result indicates that the walker is more likely to take long-range movement when the prey resource is not rich enough, which is in accordance with the experiment on the prey behavior of bumblebees [8] and also is supported by the recent observation on the movements patterns of marine predators [19]. Our result suggests that the animals living in a habitat with abundant prey resource will not display scaling property in their mobility.

As shown in the inset of Fig. 3(b), the relation between α and M can be well captured by the logarithmic form $\alpha \sim -\ln M$. The case of $M = 1$ corresponds to a solitary animal living in a fixed territory, while $M > 1$ represents the case where several animals share the prey resource in the same field. This result indicates that the individuals in a large group are more likely to make long-range movements when the resource is not sufficiently rich.

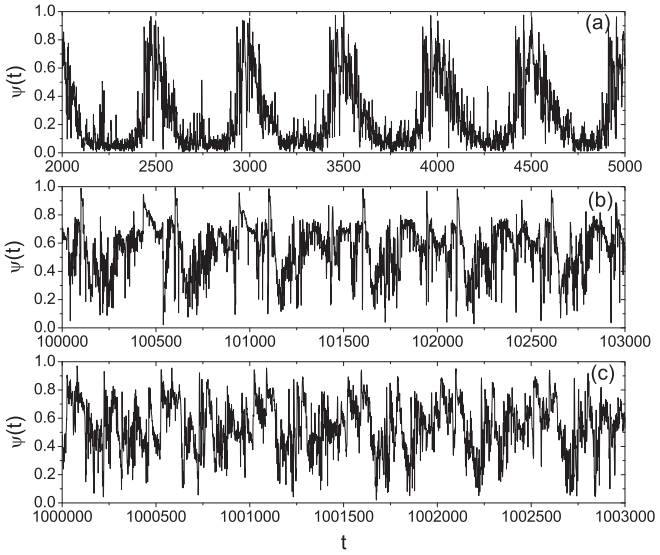

FIG. 6. The periodic varying of the order parameter $\psi(t)$ at three time periods with parameters $r = 0.99$, $M = 500$, and $N = 500$.

We also investigate the evolution process of MLD and the effect of the size of the landscape. Although the collective movements and varying patterns of the order parameter are obviously different in the early, middle, and later stages (see, for example, Fig. 6), the change in MLD is slight. As shown in Fig. 4(a), the power-law parts of MLD in different time stages are generally in parallel. After the evolution of $\frac{S}{(1.0-r)M}$ time steps (for $r = 0.99$, $M = 500$, and $N = 500$, $\frac{S}{(1.0-r)M} = 5 \times 10^4$), the MLD tends to be stable and is almost unchanged [see the green circles and the blue triangles in Fig.4(a)]. Accordingly, we set the initial time length as $\frac{S}{(1.0-r)M}$ in our simulations. When $r \to 1$, the landscape size N mainly affects the cutoff of MLD. As shown in Fig. 4(b), the cutoffs of MLD are close to N, but the slopes of the power-law parts for different N are generally the same, suggesting that the size N only limits the long-range movements but rarely affects the scaling property in the model.

IV. COLLECTIVE MOVEMENTS

To our surprise, collective movements are observed when M is large and r is close to 1, where walkers may line up one or several marching bands and walkers in the same marching band have similar moving directions (approximately perpendicular to the band). A typical example is shown in Fig. 5. Sometimes over half of the walkers are in these marching bands. Marching bands are not stable. They may suddenly emerge or disappear, may grow larger or break into pieces.

We define an order parameter $\psi(t)$ to measure the degree of synchronization of walkers' directions at time step t as the following form [20]:

$$\psi(t) = \frac{|\sum \vec{v}_i(t)|}{\sum |\vec{v}_i(t)|}, \tag{1}$$

where the velocity vector $\vec{v}_i(t) = (x_{t+1} - x_t)\hat{x} + (y_{t+1} - y_t)\hat{y}$, the coordinate (x, y) denotes the position of the ith walker, and $\hat{x}$ and $\hat{y}$ denote the unit of velocity on the x axis and y axis,

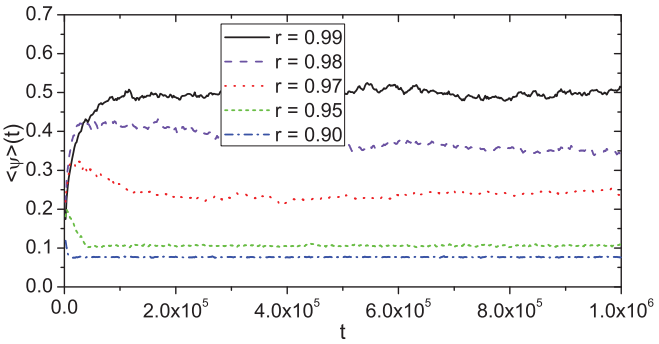

FIG. 7. (Color online) The average value in each period of the order parameter $\langle\psi\rangle(t)$ for different r, i.e., $\langle\psi\rangle(t)$ is the average value of ψ in the range $[t - \frac{S}{2M}, t + \frac{S}{2M}]$. Simulations were run with the parameter setting $M = 500$ and $N = 500$. All the data points are averaged over 20 independent runs.

respectively. Obviously, $\psi = 1$ if all walkers have the same direction.

Figure 6 reports three typical examples of the $\psi(t)$ curves for early, middle, and relatively later stages, where the quasiperiodic behavior can be observed. The period length is about S/M. As shown in Fig. 7, when $r = 0.99$, the order parameter will exceed 0.5, indicating a strong synchronization of an individual's directions. Collective movements can only be observed when r is close to 1, which is also the condition for the emergence of scaling mobility patterns, as mentioned in Sec. III. This property is demonstrated by the simulations shown in Fig. 7, where one can see that the steady value of the order parameter is very sensitive to the parameter r, and when r decreases from 1, the collective movements sharply disappear. Note that our model does not imply any direct interaction between walkers. They are driven by the coevolution of the resource landscape and the least-action movements. This feature is far different from most known interpretations on the dynamical mechanisms of animal collective movements [20–25] but is similar to the so-called active walk process [26,27], where the macroscopic-level structure emerges from the interplay between walkers and the landscape. The existence of synchronized motions is very sensitive to the value of r, suggesting that food shortage may be responsible for the emergence of animal collective behaviors, which has been observed for locusts [28]. The existence of the scaling law in the displacement distribution and the collective movements are, to our surprise, under the same condition, $r \to 1$. However, these two phenomena are not two sides of a coin; actually, they do not straightforwardly depend on each other. Whether there exists a certain mechanism underlying the coexistence is still an open question for us.

V. CONCLUSIONS AND DISCUSSIONS

Our model mimics the mobility patterns of many least-action walkers that prey in a landscape with regenerating ability. The scaling law of MLD emerges when the regeneration speed of the prey resource approaches the critical point at which the amount of resource is just enough. This result indicates that the mobility patterns of animals are

sensitive to the environmental context (e.g., food resources), which is qualitatively supported by real observations [8,19]. Our model indicates that population also highly affects the mobility patterns [see the inset of Fig. 3(b)], which is rarely discussed in early DW models. In addition, our model generates quasiperiodic collective movements with marching bands when $r \to 1$, indicating that the aggregations of animals are more likely to appear with food shortage [28,29], which is far different from many known dynamical interpretations based on the interaction between individuals [20–25]. One of the noticeable features in our results is the coexistence of both scaling mobility patterns at an individual level and collective movement at the population level. Both phenomena are under almost the same condition: the amount of prey resource approaches the critical point, implying that the environment-driven mechanism may bridge the scaling individual activity patterns and global ordered behaviors.

Under different parameter settings, our results exhibit a wide and gradual spectrum of different mobility features: from scaling movements to the random-walk-like mobility pattern and from ordered collective movements to uncorrelated motions. These results are well in agreement with different types of real-world mobility patterns of animals. However, not all the results in our model are fully addressed. Some phenomena, such as the logarithmic relation between α and M and the microscopic mechanism in the emergence of such collective movements, are still open questions for us.

As a minimum model, our model only keeps several of the most relevant factors and thus cannot mimic every detail of animal mobility. For example, the prey in our model are static and distributed in each lattice, and the mobility of prey, the heterogeneity of the distribution of resources, and the effect of the irrelevant nature are completely ignored. Some real situations, such as the extreme food shortage that occurs when the consumption of the prey resource is higher than the regeneration speed ($r > 1$), are not considered. In brief, although our model is a minimum model that ignores a few real factors, the results of our model are generally in agreement with many observations in the wild. Our model could be helpful in understanding the origin of both scaling mobility patterns and the ordered collective movements of animals.

ACKNOWLEDGMENTS

This work was supported by the National Natural Science Foundation of China Grants No. 70871082, No. 10975126, No. 70971089, and No. 10635040.

APPENDIX: MEAN-FIELD ANALYSIS

When $r \to 1$, the analysis can be simplified by the periodic movements. At the critical point, the period length is equal to S/M, and during a period, each lattice will be visited exactly once. We introduce a mean-field approximation that, at any time, the unvisited lattices are evenly distributed in the space. After τ time steps, the number of unvisited lattices is $m(\tau) = S - M\tau$. Defining the normalized move length $l_* = l/N = lS^{-1/2}$, where l is the real geometric length, the normalized probability density of the distance (move length)

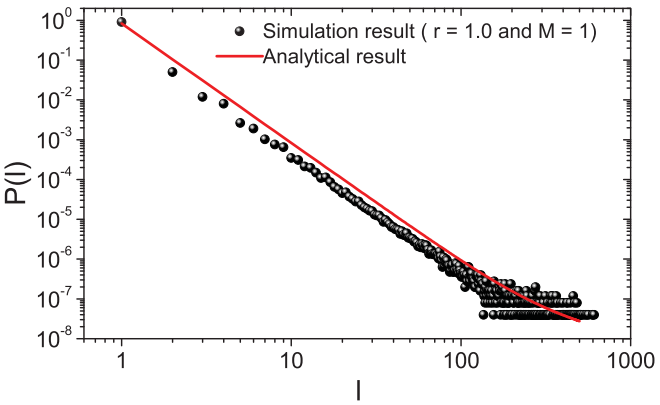

FIG. 8. (Color online) Comparison of the analytical result [Eq. (A5); red line] and the simulation result (black circles) when $r = 1$, $M = 1$, and $N = 500$. The term l^{-1} plays a role only for large l.

from an unvisited lattice to its nearest unvisited lattice after τ steps is

$$p(l_*,\tau) \approx [m(\tau) - 1] \times 2\pi l_*(1 - \pi l_*^2)^{m(\tau)-2}. \quad \text{(A1)}$$

The MLD $P(l_*)$ during a period is the cumulation of these $p(d,\tau)$:

$$P(l_*) \approx \frac{M}{S}\int_0^{S/M} p(l_*,\tau)d\tau. \quad \text{(A2)}$$

Substituting $m(\tau) = S - M\tau$ into Eqs. (A1) and (A2), $P(l_*)$ can be obtained as

$$P(l_*) \approx \frac{2\pi l_*}{S}[(\ln a)^{-2} + (\ln a)^{-1}]a^{-2}, \quad \text{(A3)}$$

where $a = 1 - \pi l_*^2$. Mostly, $l_* \ll 1$, and thus, $\ln(1 - \pi l_*^2) \approx \pi l_*^2$ and $a^{-2} \approx 1$. Therefore, $P(l_*)$ can be written as

$$P(l_*) \approx \frac{2}{S}\left(\frac{1}{\pi}l_*^{-3} + l_*^{-1}\right), \quad \text{(A4)}$$

corresponding to the distribution

$$P(l) \sim \left(\frac{S}{\pi}l^{-3} + l^{-1}\right). \quad \text{(A5)}$$

The range of l is limited to values from 1 to $\sqrt{2S}$; therefore, if S is very large, the distribution $P(l)$ is mainly determined by the first term, $\frac{S}{\pi}l^{-3}$. Figure 8 reports the analytical result, Eq. (A5), which agrees well with the simulation. Note that the term l^{-1} only shows its effect for very large l. The mean-field analysis agrees well with the simulations for small M. When M is large, the mean-field approximation will be invalidated because of the emergence of collective movement.

[1] G. M. Viswanathan, E. P. Raposo, and M. G. E. da Luz, Phys. Life Rev. **5**, 133 (2008).
[2] G. M. Viswanathan, V. Afanasyev, S. V. Buldyrev, E. J. Murphy, P. A. Prince, and H. E. Stanley, Nature (London) **381**, 413 (1996).
[3] A. M. Reynolds, Phys. Lett. A **354**, 384 (2006).
[4] A. M. Reynolds, A. D. Smith, R. Menzel, U. Greggers, D. R. Reynolds, and D. R. Riley, Ecology **88**, 1955 (2007).
[5] G. Ramos-Fernández, J. L. Mateos, O. Miramontes, G. Cocho, H. Larralde, and B. Ayala-Orozco, Behav. Ecol. Sociobiol. **55**, 223 (2004).
[6] F. Bartumeus, F. Peters, S. Pueyo, C. Marrasé, and J. Catalan, Proc. Natl. Acad. Sci. USA **100**, 12771 (2003).
[7] D. W. Sims, E. J. Southall, N. E. Humphries, G. C. Hays, C. J. A. Bradshaw, J. W. Pitchford, A. James, M. Z. Ahmed, A. S. Brierley, M. A. Hindell, D. Morritt, M. K. Musyl, D. Righton, E. L. C. Shepard, V. J. Wearmouth, R. P. Wilson, M. J. Witt, and J. D. Metcalfe, Nature (London) **451**, 1098 (2008).
[8] G. M. Viswanathan, S. V. Buldyrev, S. Havlin, M. G. E. da Luzk, E. P. Raposok, and H. E. Stanley, Nature (London) **401**, 911 (1999).
[9] F. Bartumeus, J. Catalan, U. L. Fulco, M. L. Lyra, and G. M. Viswanathan, Phys. Rev. Lett. **88**, 097901 (2002).
[10] A. M. Reynolds, Phys. Lett. A **360**, 224 (2006).
[11] M. A. Lomholt, T. Koren, R. Metzler, and J. Klafter, Proc. Natl. Acad. Sci. USA **105**, 11055 (2008).
[12] D. Boyer, O. Miramontes, G. Ramos-Fernández, J. L. Mateos, and G. Cocho, Phys. A **342**, 329 (2004).
[13] M. C. Santos, D. Boyer, O. Miramontes, G. M. Viswanathan, E. P. Raposo, J. L. Mateos, and M. G. E. da Luz, Phys. Rev. E **75**, 061114 (2007).
[14] A. M. Reynolds, Phys. Rev. E **78**, 011906 (2008).
[15] D. Boyer, O. Miramontes, and H. Larralde, J. Phys. A **42**, 434015 (2009).
[16] A. M. Reynolds, Phys. Rev. E **72**, 041928 (2005).
[17] D. Boyer, G. Ramos-Fernández, O. Miramontes, J. L. Mateos, G. Cocho, H. Larralde, H. Ramos, and F. Rojas, Proc. R. Soc. B **273**, 1743 (2006).
[18] A. Kamimura and T. Ohira, New J. Phys. **12**, 053013 (2010).
[19] N. E. Humphries, N. Queiroz, J. R. M. Dyer, N. G. Pade, M. K. Musyl, K. M. Schaefer, D. W. Fuller, J. M. Brunnschweiler, T. K. Doyle, J. D. R. Houghton, G. C. Hays, C. S. Jones, L. R. Noble, V. J. Wearmouth, E. J. Southall, and D. W. Sims, Nature (London) **465**, 1066 (2010).
[20] T. Vicsek, A. Czirók, E. Ben-Jacob, I. Cohen, and O. Shochet, Phys. Rev. Lett. **75**, 1226 (1995).
[21] Iain D. Couzin, J. Krause, R. James, G. D. Ruxton, and N. R. Franks, J. theor. Biol. **218**, 1 (2002).
[22] Iain D. Couzin, J. Krause, N. R. Franks, and S. A. Levin, Nature (London) **433**, 513 (2005).
[23] M. Ballerini, N. Cabibbo, R. Candelier, A. Cavagna, E. Cisbani, I. Giardina, V. Lecomte, A. Orlandi, G. Parisi, A. Procaccini, M. Viale, and V. Zdravkovic, Proc. Natl. Acad. Sci. USA **105**, 1232 (2008).
[24] M. Nagy, Z. Ákos, D. Biro, and T. Vicsek, Nature (London) **464**, 890 (2010).
[25] H.-T. Zhang, M. Z. Q. Chen, G.-B. Stan, T. Zhou, and J. M. Maciejowski, IEEE Circuits Syst. Mag. **8**, 67 (2008)
[26] L. Lam, Int. J. Bifurcat. Chaos Appl. Sci. Eng. **15**, 2317 (2005).
[27] L. Lam, Int. J. Bifurcat. Chaos Appl. Sci. Eng. **16**, 239 (2006).
[28] J. Buhl, D. J. T. Sumpter, I. D. Couzin, J. J. Hale, E. Despland, E. R. Miller, and S. J. Simpson, Science **312**, 1402 (2006).
[29] M. Hendrata and B. Birnir, Phys. Rev. E **81**, 061902 (2010).